ISSN 1392–1320 MATERIALS SCIENCE (MEDŽIAGOTYRA). Vol. 11, No. 1. 2005

Development of SOFC Thin Film Electrolyte Using Electron Beam Evaporation Technique from the Cubic Phase YSZ Powder

Giedrius LAUKAITIS*, Julius DUDONIS

Physics Department, Kaunas University of Technology, Studentų 50, LT-51368 Kaunas, Lithuania

Received 10 October 2004; accepted 19 October 2004

Formation of YSZ (yttrium stabilized zirconium oxide) thin films using electron beam (e-beam) physical vapor deposition technique was studied. The influence of substrate crystalline structure on growth of deposited YSZ thin film was analyzed. The YSZ thin films (1.5 – 2 μm thicknesses) were deposited on three different types of substrates: Al_2O_3, optical quartz (SiO_2), and Alloy 600 (Fe-Ni-Cr). Cubic phase ZrO_2 stabilized by 8 % of Y_2O_3 (8 % of YSZ) ceramic powder was used as evaporation material. The substrate temperature was changed in the range of 20 °C – 600 °C and its influence on the crystallinity of deposited YSZ thin films was analyzed. It was found that the substrate has no influence on the crystal orientation of the formed YSZ thin films. The dominant orientation of texture of YSZ thin films is cubic (111) and keeping the same with different types of substrate. The crystallite size varied between 20 – 40 nm and increased linearly with substrate temperature.

Keywords: YSZ thin films, fuel cells, solid oxide fuel cell (SOFC), e-beam deposition, PVD.

1.INTRODUCTION

Fuel cells (FC) technology offers many advantages over conventional methods of power generation, including higher efficiencies and negligible emissions. There are many types of fuel cells, such as: Alkaline (AFC), Direct methanol (DMFC), Phosphoric acid (PAFC), Sulphuric acid (SAFC), Proton-exchange membrane (PEMFC), Molten carbonate (MCFC), Solid oxide (SOFC), Protonic ceramic (PCFC), and etc. [1]. Solid oxide fuel cells (SOFC) present special interest because of their high operation temperature, allowing flexibility in choice of fuel, such as carbon-based fuels, e.g., natural gases. Various fuel options, such as: methane, methanol, ethanol, biogas, and gasoline are considered feasible for SOFC operation, offering in fact a very significant ecological dimension in the problem of effective energy conversion [2 – 5]. SOFC have a modular and solid state construction and do not present any moving parts, thereby are quiet enough to be installed indoors [6 – 8]. SOFC do not have the problems with electrolyte management (liquid electrolytes, for example, are corrosive and difficult to handle) and do not contain noble metals that could be problematic in resource availability and price issue in high volume manufacture [6 – 9]. SOFC have extremely low emissions for eliminating the danger of carbon monoxide in exhaust gases, as any produced CO is converted to CO_2 at the high operating temperature and have potential long life expectancy for more than 40000 – 80000 h. Also the high operating temperature of SOFC produces good quality heat byproducts that can be used for co-generation, or for use in combined cycle applications. For these many reasons SOFC are considered to be one of the most promising energy converters in the future [5].

The widespread commercialization of the SOFC will depend greatly on lowering material costs and achieving even greater gains in efficiency [8 – 10]. SOFC differ in many respects from the other fuel cells technology. First, they are composed of all-solid-state materials. Second, the cells can operate at temperature as high as 1000 °C, significantly hotter than any other major category of the fuel cells. Third, the solid state character of all SOFC components means that there is no fundamental restriction on the cell configuration. Cells are being constructed in two main configurations, i.e. tubular cells or rolled tubes, and flat-plates (planar) [2, 6, 8].

SOFC consist of two electrodes sandwiched around a hard ceramic electrolyte [2]. Electrolyte and its material has one of the basic parts and biggest influence for the SOFC performance. Different types of materials as electrolyte in the SOFC could be used yttrium- stabilized zirconium oxide- $(ZrO_2)_{0.92}(Y_2O_3)_{0.08}$ – YSZ (also could be used other stabilizing ZrO_2 dopants such as CaO, MgO, Sc_2O_3 and certain rare earth oxides such as Nd_2O_3, Sm_2O_3, Yb_2O_3); Cerium oxide doped with samarium (SDC - $Ce_{0.85}Sm_{0.15})O_{1.925}$), gadolinium (GDC - $(Ce_{0.90}Gd_{0.10})O_{1.95}$), Calcium (CDC - $(Ce_{0.88}Ca_{0.12})O_{1.88}$); yttrium doped Ceria (YDC - $(Ce_{0.85}Y_{0.15})O_{1.925}$); Lanthanum gallate ceramic including lanthanum strontium gallium magnesium (LSGM - $(La_{0.80}Sr_{0.20})(Ga_{0.90}Mg_{0.10})O_{2.85}$ or $(La_{0.80}Sr_{0.20})(Ga_{0.80}Mg_{0.20})O_{2.80}$; Bismuth yttrium oxide (BYO- $(Bi_{0.75}Y_{0.25})_2O_3$); Barium Cerate (BCN - $Ba(Ce_{0.95}Yb_{0.05})O_3$); Strontium Cerate (SYC - $Sr(Ce_{0.95}Yb_{0.05})O_3$ and etc. [6 – 11]. At present, yttria-stabilized zirconia (YSZ) cermets are the most widely adopted materials for SOFC electrolytes. It is conditioned by low YSZ electrolyte price, good thermal properties (cause by high operating temperature), and ionic conductivity. YSZ electrolyte can be fabricated in different ways: using pressing-heating technique [2], aques tape casting [12], chemical vapor deposition (CVD) [13], flame assisted vapor deposition [14], and physical vapor deposition (PVD) techniques, such as: arc discharge deposition, DC sputtering and e-beam deposition [15 – 20].

One of the ways for the lowering the cost and increasing the performance of SOFC is to use as much as

*Corresponding author. Tel.: +370-37-300349; fax: +370-37-456472.
E-mail address: *gielauk@ktu.lt* (G. Laukaitis)

possible thinner electrolyte layers (that is lowering the working temperature of the SOFC and the costs of the other components of FC). Moreover, the electrolyte should be made not porous (with cubic crystal orientation giving better ionic conductivity) on the porous substrates [2]. The shortcut between anode and cathode is the second problem. That has the influence on the electrolyte thickness (by now it is 2 – 3 μm of range).

Physical vapor deposition could be one of the best techniques for solving those requirements. It is easier to control thin film properties using PVD technology, compare to other technique.

In the present study, YSZ electrolyte thin films were deposited using e-beam deposition technique operating deposition parameters in order to get YSZ thin films that satisfy SOFC electrolyte requirements.

2. EXPERIMENTAL

YSZ thin films (1.5 – 2 μm of thicknesses) were deposited on three different substrates: Al_2O_3, optical quartz (SiO_2), and Alloy 600 (Fe-Ni-Cr) at different temperatures. The samples were cleaned in the ultrasonic bath (acetone solution) before deposition. ОІНЭ – 7 – 004 PVD (e-beam deposition technique) system was used. More details of the technical parameters of the used technique are presented in Table 1. Cubic phase Yttria-stabilized Zirconia (YSZ – 8 % mol. Y_2O_3) submicron powder was used as evaporation material. The schematic view of the experimental equipment is shown in Fig. 1. Residual gas pressure in the vacuum chamber was 4×10^{-3} Pa. The distance between electron gun and substrate was fixed at 240 mm. The substrate was additionally heated by a sample heater to temperatures from 20 °C to 600 °C. The deposition rate was evaluated from the thin film thickness measurements.

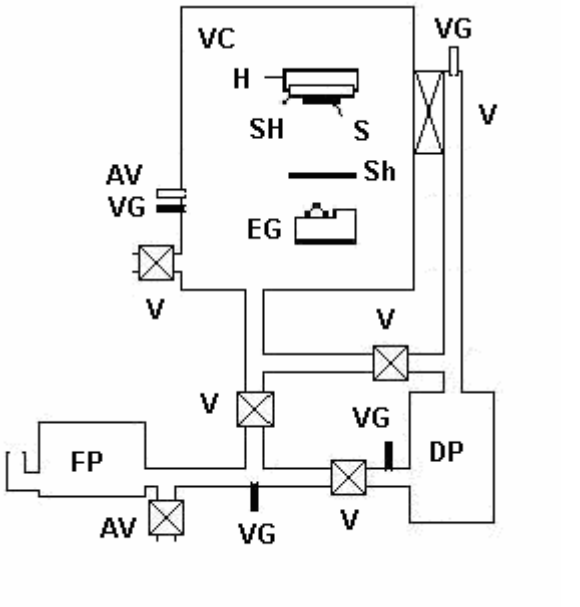

Fig. 1. PVD equipment: VC – vacuum chamber, H – sample heater, SH – sample holder with thermocouple, S – sample, EG – electrons gun, DP – diffusion pump, FP – mechanical pump, V – valves, Sh – shutter, VG – vacuum gauges, AV – air valve

Table 1. Properties of the PVD equipment

Evaporation type	E-beam evaporation (gun is cooled by water)
Pressure in the vacuum chamber	$1.3\times10^{-2} \div 6.65\times10^{-4}$ Pa
Emission current	0 ÷ 1.5A
Ionic current	0 ÷ 8 μA
Electron bending angle	270°
Power of electron gun	≤12 kW, when 8 kV voltage is used

The film structure was analyzed by X-ray diffraction (XRD) (DRON-UM1 with standard Bragg-Brentan focusing geometry) with the 2Θ angle in the range of 10 – 80° using Cu K_α radiation in steps of 0.02°. Crystallite size d of YSZ thin films was estimated from the Scherrer's equation:

$$d = 0.9\lambda/(\beta\cos\Theta), \quad (1)$$

neglecting the microstrain, where λ is the X-ray wavelength (0.154247 nm), Θ the Bragg diffraction angle, and β the full-width of peaks at half maximum intensity. The results from XRD were quantified by defining a simple texture coefficient R [21] which is the ratio of the intensities of the (111) peak to the sum of the intensities of all peaks. As the spectra consisted of (111), (200), (220), (311), (222) peaks, the coefficient becomes:

$$R_{111} = I_{111}/(I_{111} + I_{200} + I_{220} + I_{311} + I_{222}) . \quad (2)$$

The value $R = 0.57$ corresponds to the random orientation, and $R = 1$ means preferred (111) orientation.

3. RESULTS AND DISCUSSIONS

As it is mentioned in the [22 – 26], the best ionic conductivity is registered when the YSZ electrolyte crystalline orientation is (111) and ZrO_2 is stabilized to 8 – 10 % of Y_2O_3. YSZ thin films were deposited from cubic phase ZrO_2 stabilized by 8 % of Y_2O_3 (8 % of YSZ) ceramic powder. Before deposition YSZ powder was pressed to the pallets of 25 mm diameter and 2 mm of thickness. The XRD diffraction patterns of the pressed YSZ powder are presented in Fig. 2. It shows that the positions of the Bragg peaks are typical for the cubic 8 % of YSZ.

The growth rate of the film during PVD has influence on the crystallite size of the deposited YSZ thin films. For controlling the crystallite size it is necessary to know growth rate dependence on the e-beam gun power. The growth rate dependence on the e-beam gun power (Fig. 3.) shows that increasing e-beam power the growth rate increases linearly. It could be changed in the range from 0.6 nm/s to 2.0 nm/s. The PVD deposited YSZ films have good adherence to substrate. For lower rates (<1.5 nm/s) the films appear as uniform, shiny, and mirror-like. At higher e-beam power, when the growing rate is higher than 1.5 nm/s, deposition process is going to be unstable. The material is evaporated in big clusters and the thin film starts to be nonhomogeneous with bad adhesion to the substrate.

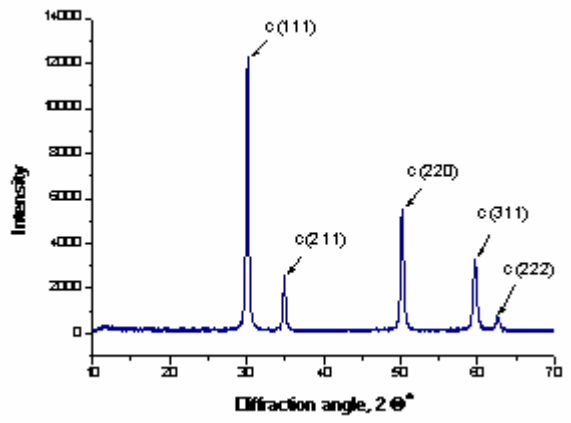

Fig. 2. XRD patterns of pressed ceramic powder of cubic phase ZrO_2 stabilized by 8 % Y_2O_3 (8 % YSZ)

Three types of materials: crystalline (Alloy 600, Fe-Ni-Cr), polycrystalline (Al_2O_3), and amorphous (optical quartz, SiO_2) substrates were chosen in order to understand the influence of substrate material on the crystal orientation of deposited YSZ thin film using e-beam deposition technique. XRD diffraction patterns show (Fig. 4) that substrate does not influence on the crystal orientation of the YSZ thin film. The dominant thin films crystal orientation was cubic (111) (Fig. 4) and keeping the same for different types of substrate. The sharpness of (111) XRD peaks indicates high degree of homogeneity of YSZ thin films. YSZ thin films exhibit minor (200), (220), (311) and (222) orientation also. Deposited YSZ thin films repeat the crystal orientation of the chosen evaporated material. YSZ thin films crystal orientation corresponds to the requirements for good ionic conductivity of YSZ electrolytes [22 – 26]. Using other PVD techniques the substrate has big influence on the orientation and crystallinity of YSZ thin film, especially when reactive sputtering [27] is used.

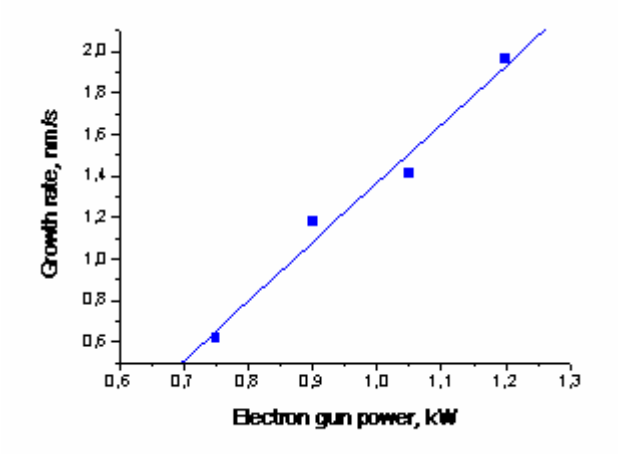

Fig. 3. YSZ thin films growth rate dependence on the e-gun power

The substrate temperature has no influence on orientation of the YSZ thin film (Fig. 5) as is presented when using CVD technique [13]. The temperature does not influence the crystal orientation when thin film is deposited on the different type of substrates. The main crystal orientation does not change increasing temperature, but the crystallite size increases (Fig. 6) with the growth of deposition temperature. Fig. 6 shows that the substrate has influence on the crystallite size of the YSZ thin film. Crystallite size is increased from 150 nm to 380 nm for SiO_2 and Al_2O_3 substrates. For Alloy 600 substrate it increases from 270 nm to 420 nm. The lowest crystallite size is found to be for the substrate temperature equal to 200 °C (for all types of substrates).

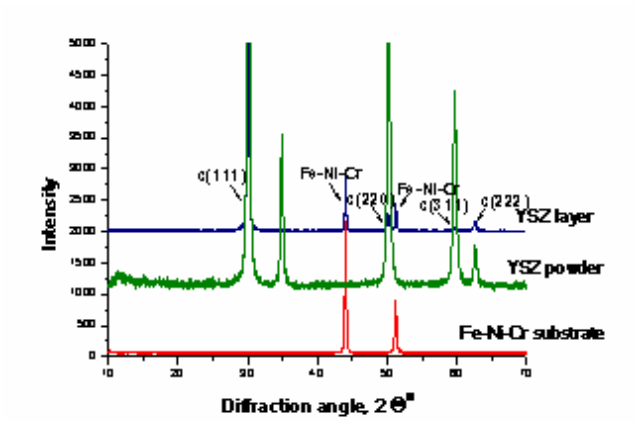

a

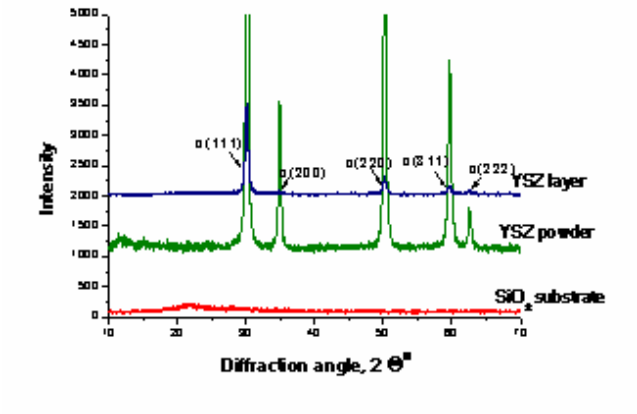

b

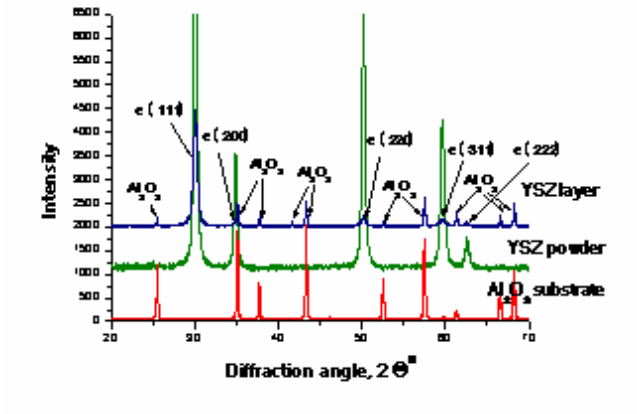

c

Fig. 4. XRD patterns of YSZ thin films deposited on Fe-Ni-Cr (a), SiO_2 (b) and Al_2O_3 (c) substrates

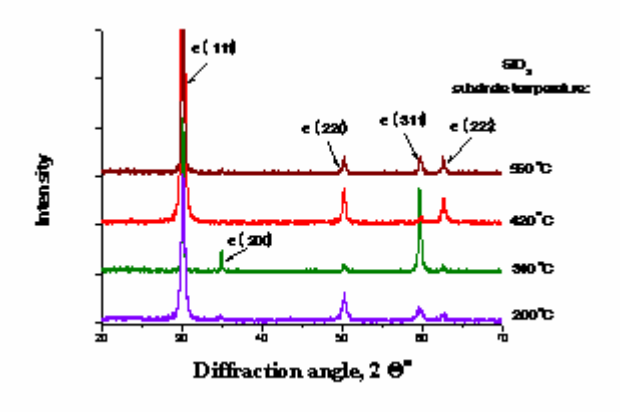

Fig. 5. XRD patterns of YSZ thin films deposited on SiO_2 different temperature substrates

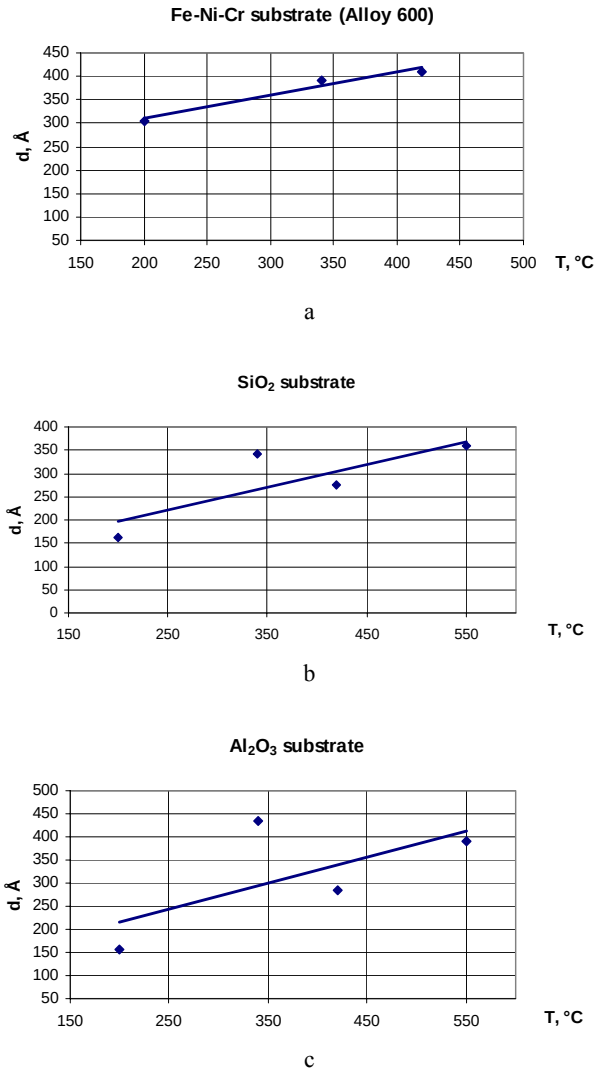

Fig. 6. YSZ thin film crystallites size (extracted from XRD data) dependence on Fe-Ni-Cr (Alloy 600) (a), SiO_2 (b) and Al_2O_3 (c) substrates temperature T

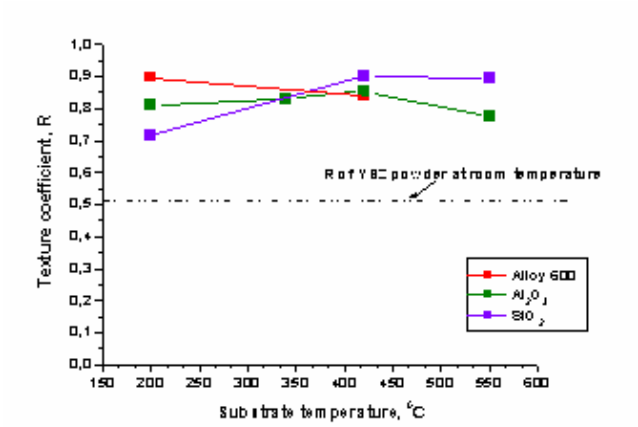

Fig. 7. YSZ thin films texture coefficient R dependence on the substrate (Fe-Ni-Cr (Alloy 600), Al_2O_3, SiO_2) temperature

Fig. 7 shows the texture coefficient as a function of substrate temperature during the deposition of YSZ thin films. The films grow with preferred (111) orientation at for all type of substrates (Al_2O_3, optical quartz (SiO_2), Alloy 600 (Fe-Ni-Cr)). The texture (111) dominates in the substrate temperature region (200 – 550 °C).

4. CONCLUSIONS

The growth rate dependence on the e-beam gun power is linear. The deposition rate could be changed in the range from 0.6 nm/s to 2.0 nm/s. The substrate has no influence on the crystal orientation of the formed YSZ thin films. The dominant orientation of texture of thin films is cubic (111) for different types of substrates (Alloy 600, Fe-Ni-Cr, Al_2O_3 and optical quartz – SiO_2) while evaporating 8% of YSZ ceramic powder. The texture (111) dominates in the substrate temperature region (200 °C – 550 °C). The crystallite size varied between 20 – 40 nm and increased linearly with substrate temperature.

Acknowledgement

Lithuanian State Science and Studies Foundation have supported this work and Lithuanian Energy Institute for help with experimental measurements.

REFERENCES

1. **Haile, S. M.** Fuel Cell Materials and Components *Acta Materialia* 51 2003: pp. 5981 – 6000.
2. **Larminie, J., Dicks, A.** Fuel Cells Systems Explained. John Wiley & Sons Ltd., 2003: 406 p.
3. **Douvartzides, S., Coutelieris, F., Tsiakaras, P.** Exergy Analysis of a Solid Oxide Fuel Cell Power Planted by Either Ethanol or Methane *Journal of Power Sources* 131 Issues 1 – 2 2004: pp. 224 – 230.
4. **Coutelieris, F. A., Douvartzides, S., Tsiakaras, P.** The Importance of the Fuel Choice on the Efficiency of a Solid Oxide Fuel Cell System *Journal of Power Sources* 123 2003: pp. 200 – 205.

5. **Jan Van Herle, Membrez, Y., Bucheli, O.** Biogas as a Fuel Source for SOFC Co-generators *Journal of Power Sources* 127 Issues 1 – 2 2004: pp. 300 – 312.
6. **Masayuki Dokiya.** SOFC System and Technology *Solid State Ionics* 152 – 153 2002: pp. 383 – 392.
7. **Fukushima, Y., Shimada, M., Kraines, S., Hirao, M., Koyama, M.** Scenarios of Solid Oxide Fuel Cell Introduction into Japanese Society *Journal of Power Sources* 131 Issues 1 – 2 2004: pp. 327 – 339.
8. **Boudghene Stambouli, A., Pravers, E.** Solid Oxide Fuel Cells (SOFCs): a Review of an Environmentally Clean and Efficient Source of Energy *Renewable and Sustainable Energy Reviews* 6 2002: pp. 433 – 455.
9. **Tu, H., Stimming, U.** Advances, Aging Mechanisms and Lifetime in Solid-oxide Fuel Cells *Journal of Power Sources* 127 2004: pp. 284 – 293.
10. **Tietz, F., Buchkremer, H.-P., Stover, D.** Components Manufacturing for Solid Oxide Fuel Cells *Solid State Ionics* 152 – 153 2002: pp. 373 – 381.
11. **Dokiya, M.** SOFC System and Technology *Solid State Ionics* 152 – 153 2002: pp. 383 – 392.
12. **Snijkers, F., De Wilde, A., Mullens, S., Luyten, J.** Aques Tape Casting of Yttria Stabilized Zirconia Using Natural Product Binder *Journal of the European Ceramic Society* 24 2004: pp. 1107 – 1110.
13. **Wang, H. B., Xia, C. R., Meng, G. Y., Peng, D. K.** Deposition and Characterization of YSZ Thin Films by Aaerosol-assisted CVD *Materials Letters* 44 2000: pp. 23 – 28.
14. **Charojrochkul, S., Choy, K. L., Steele, B. C. H.** Flame Assisted Vapour Deposition of Cathode for Solid Oxide Fuel cells: 1. Microstructure Control from Processing Parameters *Journal of the European Ceramic Society* 24 2004: pp. 2515 – 2526.
15. **Wanzenberg, E., Tietz, F., Kek, D., Panjan, P., Stover, D.** Influence of Electrode Contacts on Conductivity Measurements of Thin YSZ Electrolyte Films and the Impact on Solid Oxide Fuel Cells *Solid State Ionic,s* 164 2003: pp. 121 – 129.
16. **Horita, S., Nakajima, H., Kuniya, T.** Improvement of the Electrical Properties of Heteroepitaxial Yttria-stabilized Zirconia (YSZ) Films on Si Prepared by Reactive Sputtering *Vacuum* 59 2000: pp. 390 – 396.
17. **Nagata, A., Okayama, H.** Characterization of Solid Oxide Fuel Cell Device having a Three-layer Film Structure Grown by RF Magnetron Sputtering *Vacuum* 66 2002: pp. 523 – 529.
18. **Caricato, A. P., Di Cristoforo, A., Fernandez, M., Leggieri, G., Luches, A., Majni, G., Martino, M., Mengucci, P.** Pulsed Excimer Laser Ablation Deposition of YSZ and TiN/YSZ Thin Films on Si Substrates *Applied Surface Science* 208 – 209 2003: pp. 615 – 619.
19. **Ju Hyung Suh, Sang Ho Oh, Hyung Seok Kim, Se-Young Choi, Chan-Gyung Park, C.-G.** Effects of Neutralizers on the Crystal Orientation of YSZ Films Grown by Using Ion Beam Sputtering *Vacuum* 74 Issues 3 – 4 2004: pp. 423 – 430.
20. **Nicholls, J. R., Deakin, M. J., Rickerby, D. S.** A Comparison Between the Erosion Behaviour of Thermal Spray and Electron Beam Physical Vapour Deposition Thermal Barrier Coatings *Wear* 233 – 235 1999: pp. 352 – 361.
21. **Ensinger, W.** Low Energy Ion Assist During Deposition – an Effective Tool for Controlling Thin Film Microstructure *Nuclear Instruments and Methods in Physics Research B* 127/128 1997: pp. 769 – 808.
22. **Craig Fisher, A. J., Matsubara, H.** The Influence of Grain Boundary Misorientation on Ionic Conductivity in YSZ *Journal of the European Ceramic Society* 19 1999: pp. 703 – 707.
23. **Pramananda Perumal, T., Sridhar, V., Murthy, K. P. N., Easwarakumar, K. S., Ramasamy, S.** Molecular Dynamics Simulations of Oxygen Ion Diffusion in Yttria-stabilized Zirconia *Physica A* 309 2002: pp. 35 – 44.
24. **Fisher, C. A. J., Matsubara, H.** Oxide Ion Diffusion Along Grain Boundaries in Zirconia: A Molecular Dynamic Study *Solid State Ionics* 113 – 115 1998: pp. 311 – 318.
25. **Ostanin, S., Craven, A. J., McComb, D. W., Vlachos, D., Alavi, A., Paxton, A. T., Finnis, M. W.** Electron Energy-loss Near-edge Shape as a Probe to Investigate the Stabilization of Yttria-stabilized Zirconia *Physical Review B* 65 2002: 224109
26. **Skib Khan, M., Saiful Islam, M., David Bates, R.** Cation Doping and Oxygen Diffusion in Zirconia: a Combined Atomistic Simulation and Molecular Dynamic Study *J. Mater. Chem.* 8 (10) 1998: pp. 2299 – 2307.
27. **Hata, T., Sasaki, K., Ichikawa, Y., Sasaki, K.** Yttria-stabilized Zirconia (YSZ) Heteroepitaxially Grown on Si Substrates by Reactive Sputtering *Vacuum* 59 2000: pp. 381 – 389.